Solid Earth Discuss., 6, 1523–1554, 2014
www.solid-earth-discuss.net/6/1523/2014/
doi:10.5194/sed-6-1523-2014

Solid Earth
Discussions
Open Access

Using the level set method in geodynamical modeling of multi-material flows and Earth's free surface

B. Hillebrand[1], C. Thieulot[1,2], T. Geenen[3], A. P. van den Berg[1], and W. Spakman[1,2]

[1]Department of Earth Sciences, Utrecht University, the Netherlands
[2]Centre of Earth Evolution and Dynamics (CEED), University of Oslo, 0316 Oslo, Norway
[3]SurfSara, Amsterdam, the Netherlands

Received: 4 June 2014 – Accepted: 10 June 2014 – Published: 9 July 2014

Correspondence to: B. Hillebrand (b.hillebrand@uu.nl)

Published by Copernicus Publications on behalf of the European Geosciences Union.

Abstract

The level set method allows for tracking material surfaces in 2-D and 3-D flow modeling and is well suited for applications of multi-material flow modeling. The level set method utilizes smooth level set functions to define material interfaces, which makes the method stable and free of oscillations that are typically observed in case step-like functions parameterize interfaces. By design the level set function is a signed distance function and gives for each point in the domain the exact distance to the interface and on which side it is located. In this paper we present four benchmarks which show the validity, accuracy and simplicity of using the level set method for multi-material flow modeling. The benchmarks are simplified setups of dynamical geophysical processes such as a Rayleigh–Taylor instability, post glacial rebound, subduction and slab detachment. We also demonstrate the benefit of using the level set method for modeling a free surface with the sticky air approach. Our results show that the level set method allows for accurate material flow modeling and that the combination with the sticky air approach works well in mimicking Earth's free surface. Since the level set method tracks material interfaces instead of materials themselves, it has the advantage that the location of these interfaces is accurately known and that it represents a viable alternative to the more commonly used tracer method.

1 Introduction

Accurate modeling of geodynamical processes involving large deformation, e.g. mantle flow, subduction evolution or slab tearing, is a key research goal in computational geodynamics. Since the early simplified two-dimensional isothermal model configurations (Gurnis and Hager, 1988; Christensen, 1996) model complexity and especially the number of materials present in numerical models have dramatically increased as seen in recent three-dimensional thermo-mechanically coupled models that include multiple materials and phase changes as well as surface deformation and complex rheologies. (e.g. van Hunen and Allen, 2011; Duretz et al., 2014). For instance multiple materials are important to investigate the influence of an oceanic crust on the decoupling of subducting and overriding plates as well as on the buoyancy of the subducting slab (Běhounková and Čižková, 2008; van Hunen and van den Berg, 2008; Androvičová et al., 2013), they are also important for research involving subduction termination by continental collision (e.g., Baumann et al., 2010; Magni et al., 2012). Other studies focus on the influence of complex rheologies on slab dynamics (Billen and Hirth, 2007; Andrews and Billen, 2009) and finally to investigate the influence and response of a free surface in subduction modeling has been the aim of many recent studies (e.g., Schmeling et al., 2008; Gerya et al., 2009; Quinquis et al., 2011; Duretz et al., 2011).

The models described above invariably require the ability to track different materials and material interfaces throughout the model domain. Within the community several different methods, based on either Langrangian or Eulerian modeling frameworks, are used. In Lagrangian finite element codes the mesh is deformable and element boundaries are often aligned with the material interfaces. The elements thus track the materials through the model. However when large deformation is modeled, e.g. when following subduction evolution the mesh may become too distorted and remeshing is required. This is computationally expensive and results in unwanted numerical diffusion and constitutes an important drawback for models with large deformation.

In Eulerian codes the mesh is fixed. Because of this elements do not track materials and a method for material tracking is needed. The two more commonly used methods in computational geodynamics, are the marker-in-cell technique and the phase field method.

Tracers (particles, markers) are widely used in the geodynamical community (e.g., Tackley and King, 2003; van Hunen and Allen, 2011; Duretz et al., 2012). These Lagrangian particles are advected with the flow and carry material properties such as for example density and viscosity. Velocity equations are solved on the finite element mesh and the velocities used to advect the particles are obtained from interpolation. One element generally contains several up to 100's of particles. This method easily allows for advection of multi-material fields using an Eulerian mesh and is potentially non diffusive (Tackley and King, 2003). However the tracer method tracks materials, it does not track the interface between the materials. The interface position remains approximate and is known with an uncertainty of the order of local tracer distance. Furthermore, the tracer method becomes increasingly expensive in 3-D. For instance in the 2-D models of Crameri et al. (2012) the different codes use between ten up to hundreds of particles per element/cell. In 3-D this translates to several dozens up to thousands of particles per element/cell i.e. possibly billions in total in the case of large 3-D simulations. The computational as well as the memory costs would then become huge requiring that the code is highly parallel and scales up to hundreds of cores or more.

In the phase field method (Lenardic and Kaula, 1993; Van Keken et al., 1997; Kronbichler et al., 2012), materials are assigned a number, and the composition of the fluid at a given node of the grid is given by a field containing the various fractions of the different material components. This field is then advected using a stabilized advection equation. The phase field vector is only defined on the nodal points of the mesh thus the computational costs increase proportionally to the increase in nodal points. However such a phase field will contain sharp contrasts between the different phases within elements and the advection of the phase field requires complex stabilization schemes (Lenardic and Kaula, 1993).

In this paper we explore a third method, the level set method, that, instead of tracking materials is geared to track the material interfaces. The method is based on defining a level set function (generally signed distance) which is zero at the target interface and positive on one side and negative on the other side. This "signed" property is used to identify the different materials. Similar to the phase field method the level set function is defined on the nodal points of the elements and the computational costs increase proportional to the increase in nodal points. In contrast with the phase field method, the level set method does not involve step-like discontinuities but instead represents fields with a smooth (signed distance) function (the level set function). As a direct conse-

SED
6, 1523–1554, 2014

quence the advection scheme need not be of high order. The level set method has not often been used in the geodynamical community with the notable exceptions of Zlotnik et al. (2008); Braun et al. (2008) and Hale et al. (2010). In the case of Braun et al. (2008) the level set method is based on a 3-D set of triangulated points, which makes it a hybrid between tracers and level set functions. The level set method is primarily used in other fields of computational science such as two-phase flows (Oka and Ishii, 1999) and fluid dynamics (Rao et al., 2011). An overview of the method and applications can be found in Osher and Fedkiw (2001).

In this paper we present four benchmarks of increasing complexity and end with applications to modeling of subduction and slab detachment. Two of the presented benchmarks include deformation of Earth's free surface. In Eulerian based codes this is generally modeled either by ALE (Arbitrary Langrangian Eulerian, Fullsack, 1995; Thieulot, 2011) methods or the so-called sticky air approach (Schmeling et al., 2008; Crameri et al., 2012). In ALE the top layers of elements can deform vertically. The sticky air approach entails that an "air" layer of low viscosity and zero density is put atop the surface. This causes the Earth's surface to become a boundary between two materials inside the model domain which we track using the level set method.

The purpose of our paper is to demonstrate the use of the level set method in various geodynamic applications and to demonstrate the applicability of the presented approach to more complex geodynamical processes.

2 Methods

All experiments in this paper are mechanical models internally driven by density perturbations. They do not include any temperature effects. We use the finite element modeling package SEPRAN (Segal and Praagman, 2005) and solve for mass conservation of an incompressible fluid,

$$\nabla \cdot \boldsymbol{v} = 0 \tag{1}$$

and the Stokes equation describing a force balance:

$$-\nabla P + \nabla \cdot \boldsymbol{\sigma}_\mathrm{d} = \boldsymbol{f}(\rho) \tag{2}$$

Here $\boldsymbol{v}$ is velocity, P dynamic pressure, ρ density and $\boldsymbol{\sigma}_\mathrm{d}$ the deviatoric stress tensor. In all benchmarks the density is a function of the material that is advected through the domain which is tracked by means of the level set method. The modeling package SEPRAN has been used in geodynamical modeling for many years (Čížková et al., 2007; van Hunen and van den Berg, 2008; Chertova et al., 2012; Androvičová et al., 2013, e.g.).

2.1 Level set method

The level set method was devised by Osher and Sethian (1988). It tracks an interface by defining it as the zero valued isocontour of a smooth function. This function is called the level set function. If Γ denotes the interface that is to be associated and tracked with a level set function ϕ and Ω is a bounded region, bounded by just the interface or the interface and the boundaries of the model domain, then ϕ is defined as (Osher and Fedkiw, 2001):

$$\begin{aligned} &\phi(r,t) > 0 \quad \text{for } r \in \Omega \\ &\phi(r,t) < 0 \quad \text{for } r \notin \Omega \\ &\phi(r,t) = 0 \quad \text{for } r \in \partial\Omega = \Gamma(t) \end{aligned} \tag{3}$$

The level set function is advected by means of the advection equation:

$$\frac{\partial \phi}{\partial t} + \boldsymbol{v} \cdot \nabla \phi = 0 \tag{4}$$

This equation is solved using a Crank–Nicolson integration scheme in combination with the SUPG upwind scheme (Brooks and Hughes, 1982). The level set function is generally chosen to be a signed distance function which means that $|\nabla \phi| = 1$ everywhere.

The function value indicates on which side of the interface a point is located (negative or positive) and this is used to identify materials. Because the level set function is a signed distance function, its value is also the distance to the interface.

2.1.1 Reinitialization

The level set function is advected with a velocity field resulting from the buoyancy forces. This velocity field does not necessarily preserve the signed distance quality of the level set function. However it has been shown by several authors (Sussman et al., 1995; Min, 2010) that it is important for the level set function to stay smooth in the vicinity of the zero level set (at least Lipschitz continuous, Osher and Fedkiw, 2001). Therefore the level set function is corrected so that it remains a smooth function without moving the zero isocontour and thus the interface itself. Sussman et al. (1995) introduced a method called reinitialization which exploits the signed distance quality of the level set function. The reinitialization process involves solving the following equation:

$$\frac{\partial \phi}{\partial \tau} = \mathrm{sign}(\phi)(1 - |\nabla \phi|) \qquad (5)$$

This equation specifies a correction for the value of ϕ if $|\nabla \phi| \neq 1$. $\partial \tau$ is a pseudo time step and $\mathrm{sign}(\phi)$ is the one dimensional signum (or sign) function, and 0 at $\phi = 0$, for which generally a smooth approximation is used. Equation (5) does not need to be solved every time step. We use an error criterion to determine whether reinitialization is needed and then solve several reinitialization iterations until our criterion is satisfied. The error is calculated by taking the average of the deviation of the absolute gradient of ϕ from 1 of all the nodal points. The number of iterations needed depends on the choice of $\partial \tau$, $\mathrm{sign}(\phi)$ and the choice of the error criterion. For the smoothened sign function we use:

$$\mathrm{sign}(\phi) = \frac{\phi}{\sqrt{\phi^2 + (C\Delta x)^2}} \qquad (6)$$

SED
6, 1523–1554, 2014
Geodynamical modeling using the level set method
B. Hillebrand et al.

The value of constant C is arbitrarily chosen. A high value results in a slower (more iterations) but more stable reinitialization process while a low value has the opposite effect. In our models $C = 15$ proved to be a practical compromise between speed and stability. The determination of $\nabla\phi$ is important for the reinitialization procedure and it needs to be robust for both small and large scale variations. We therefore use a 2nd order ENO (Essentially Non-Oscilatory) scheme for the space derivative (Osher and Shu, 1991; Jiang and Peng, 2000). We also use a 3rd order TVD (Total Variation Diminishing) Runge Kutta scheme for the pseudo time integration of Eq. (5) (Gottlieb and Shu, 1998).

2.1.2 Usage of the level set method

We use the level set method to track the interface between two different (geological) materials, but we note that the application can involve any chosen surface. Every interface is described by its own level set function. Since the level set function is defined such that its zero isocontour coincides with the interface between two materials, one material will be where the function is negative and the other where it is positive. For an arbitrary material parameter C this can be written as:

$$C = \begin{cases} C_1 & \text{for } \phi \leq 0 \\ C_2 & \text{for } \phi > 0 \end{cases} \tag{7}$$

We coin this the *sharp boundary method* which results in sharp contrasts of material parameters (density, viscosity, etc...) within an element. One can also introduce a small diffusion zone around the interface (Bourgouin et al., 2006), hereafter called the *diffuse boundary method*. It is important to note that this does not mean that the location of the interface is no longer known. The location is still exactly known.

$$C = \begin{cases} C_1 & \text{for } \phi \le -\alpha h \\ C_2 & \text{for } \phi \ge \alpha h \\ \frac{(C_2 - C_1)\phi}{2\alpha h} + \frac{(C_1 + C_2)}{2} & \text{for } |\phi| < \alpha h \end{cases} \tag{8}$$

Here $\alpha = 1$ and h represents one element size. When Eq. (8) is used to smooth density across the interface C is simply the density value, however when viscosity is smoothened across the interface C is the exponent of viscosity i.e. smoothing the logarithm of viscosity. A comparison between the two methods is performed with the Rayleigh–Taylor instability benchmark found in Sec 4. In the other benchmarks the diffuse boundary method is used. Because of the signed distance quality of the level set function the zone of the diffuse boundary ($2h$) follows directly from the level set function values and no additional steps to identify this zone are required. The width (h) of the diffuse boundary is easily changed in case more smoothness is required.

2.2 Sticky air approach

Several of the benchmark experiments we conduct will include an approximation of the Earth's free surface using the so-called "sticky-air" approach (Schmeling et al., 2008; Crameri et al., 2012). This allows modeling of topography changes while using a purely Eulerian code by augmenting the model with a top layer with so-called "sticky-air". Since Earth's surface is effectively a stress-free surface this layer of air should exert as little stress on the underlying lithosphere material as possible. Crameri et al. (2012) investigated the viscosity contrast and thickness of the sticky air layer and concluded that for a 100 km thick layer the viscosity of the air layer should be 5 orders of magnitude less than the underlying material. The density of the sticky air layer is set to zero so that it has no pressure effect on the real free surface (the sticky air lithosphere interface).

3 Benchmarks

Here we present the model setups of the various benchmarks presented in this paper. All four benchmarks describe multi-material flow models and some include the modeling of Earth's free surface by means of a sticky air layer. The benchmarks are the Rayleigh–Taylor instability from Van Keken et al. (1997), the post glacial rebound setup from Crameri et al. (2012), the free subduction benchmark from Schmeling et al. (2008) and the simplified slab detachment setup from Schmalholz (2011). The first benchmark models the overturn of a gravitationally unstable compositional layering and is often used in the geodynamical modeling community. The second and third benchmark focus on the sticky air approach. The last benchmark setup demonstrates the splitting of one material domain into two. The setups of the benchmarks are illustrated in Fig. 1 and a small description of each follows below.

3.1 Rayleigh–Taylor instability

This benchmark represents a buoyancy driven flow and (Fig. 1a) has been performed by several authors with various techniques including tracers (Van Keken et al., 1997; Tackley and King, 2003), level set method (Bourgouin et al., 2006), particle level set method (Samuel and Evonuk, 2010), phase field method (Bangerth and Heister, 2013) and a marker chain method (Van Keken et al., 1997). The benchmark describes an almost square domain of unit height and a width of 0.9142, in which a dense layer overlies a lighter layer. The interface geometry between the two layers is given by a sine function defined as $w(x) = 0.02\cos(\frac{\pi x}{\lambda}) + 0.2$ with $\lambda = 0.9142$. We will compare snapshots at regular intervals with the snapshots of the original article (Van Keken et al., 1997). We will also compare the evolution of the root mean square velocity (v_{rms}) of the entire domain over time, specifically concentrating on the timing and height of

SED
6, 1523–1554, 2014

the first peak, which coincides with the rise of the first diapir. The v_{rms} is given by:

$$v_{rms} = \sqrt{\frac{1}{V}\int \|v\|^2 \mathrm{d}v} \tag{9}$$

Here V is the volume of the domain.

3.2 Post glacial rebound

This benchmark (Fig. 1c) is used specifically to validate the sticky air approach. It describes a three layer model (air, lithosphere and mantle) with three different viscosities and two different densities (mantle and lithosphere have the same density) and therefore requires two different level set functions at the two material interfaces. The surface (top of lithosphere) has a prescribed cosine topography with a 7 km amplitude. The system relaxes over time until the topography has reduced to zero. The height of the topography at the left side of the model is measured over time and will be compared to the semi-analytical solution from the original article.

3.3 Subduction benchmark

This subduction setup (Fig. 1b) was presented as a benchmark in Schmeling et al. (2008) and this particular setup had been performed by five different codes therein. It involves three different materials: a sticky air layer, an idealized slab which subducted for a 100 km and a mantle. Due to its negative buoyancy the slab starts to develop rollback and sinks into the mantle. The original paper clearly highlighted difficulties with different choices in tracer based viscosity averaging schemes due to the entrainment of tracers, a problem we aim to avoid by using the level set method. For comparison we will focus on the depth of the slab tip with time and snapshots through time.

SED
6, 1523–1554, 2014

3.4 Slab detachment

This setup (Fig. 1d) is from Schmalholz (2011) and is being developed into a community benchmark (Thieulot et al., 2014b). It concerns a two material model setup comprising a lithosphere with a vertically hanging slab and a mantle. The two materials have different densities and different rheological parameters. Mantle material has a linearly viscous ($n = 1$, $\eta_0 = 10^{21}$ Pa s) rheology while the slab follows a power-law rheology described by:

$$\eta = \eta_0 \dot{\epsilon}^{\frac{1}{n}-1} \tag{10}$$

in Eq. (10) $\dot{\epsilon}$ is the second invariant of the strain-rate tensor. The following values are adopted: $n = 4$ and $\eta_0 = 4.75 \times 10^{11}$ Pa s. We measure the thickness D of the thinning slab over time. We present our results in the same non-dimensional form as Schmalholz (2011), i.e. non-dimensional thickness $D_\mathrm{d} = \frac{D}{D_0}$ vs. non-dimensional time $t_\mathrm{d} = \frac{t}{t_\mathrm{c}}$. D_0 is the initial thickness of the slab (80 km) and t_c is the characteristic time. This time is calculated in the following manner:

$$t_\mathrm{c} = \frac{1}{B(0.5\Delta\rho g H)^n} \tag{11}$$

g is the gravitational acceleration, $\Delta\rho$ the density contrast between slab and mantle, H the length of the hanging slab and $B = (2\eta_0)^{-n}$. The benchmark illustrates the separation of the level set field into two domains.

4 Results

4.1 Rayleigh–Taylor instability

In Fig. 2 the time evolution of both the density and level set field of a 160×160 elements model run are shown. This can be compared with Fig. 2 from Van Keken et al. (1997).

SED
6, 1523–1554, 2014

All the large-scale features (the two upwellings, the major downwellings) are captured as well as the smaller scale features such as the small wavelet just behind the front of the first upwelling (Fig. 2c and d). The evolution of the level set field illustrates the signed distance quality of the function. In Fig. 3a the root mean square velocity (v_{rms}) of the entire domain is plotted vs. time. The first peak corresponds to the first upwelling and the second smaller peak to the second upwelling. The figure shows the results of four of our models as well as results from the marker chain method from Van Keken et al. (1997). Figure 3c shows a close-up of the first peak. This close-up shows that our results are in good agreement with Van Keken et al. (1997). The first peak is a strong feature across different codes and is therefore examined more precisely in Table 1. It is compared to the marker chain method of Van Keken et al. (1997), the level set method and the particle level set method of Samuel and Evonuk (2010) and the tracer method of Thieulot et al. (2014a). Table 1 illustrates that the first peak occurs earlier with increasing resolution, and that our results resemble the marker chain results of the original paper more than the other published level set method results. However solely looking at the highest resolution models all presented studies agree on timing and height within 1 %.

Figure 3a and c shows the results of a 160 × 160 sharp boundary method run and of a diffuse boundary method run. Although the overall difference is small the diffuse boundary method has a beneficial smoothening effect (Fig. 3c). As previously stated the signed distance quality of the level set function makes such a diffuse boundary method cheap and simple.

This benchmark involves flow of an incompressible fluid. Given the large deformation of the layers, it is appropriate to test the mass conservation of the system. To this end we calculated the relative mass difference defined in Eq. (12) and plotted the results in Fig. 3b.

$$M_{\text{rel}} = \frac{M_0 - M(t)}{M_0} \tag{12}$$

SED
6, 1523–1554, 2014

Where M_0 is the mass of the entire model domain at $t = 0$. Over time the models exhibit a variation in total mass. At $t = 2000$ the relative mass difference is still negligible (between 0.003 % and 0.0005 %). For the higher resolution models there is also no systematic mass variation visible. We therefore can state that our implementation of the level set method is mass conservative.

4.2 Post glacial rebound

Crameri et al. (2012) concluded that for a correct modeling of Earth's free surface by means of the sticky air approach the sticky air layer should either have a 5 orders of magnitude viscosity contrast with the underlying material and be 100 km thick or have a 4 orders viscosity contrast and be 200 km thick. In Fig. 4a we show results of a model which has a 100 km thick layer and five orders of magnitude difference in viscosity ($\eta_{\text{air}} = 10^{18}$ Pa s) with the lithosphere. The grey area illustrates that the topography error of our model results never exceed 100 m. These results illustrate to our knowledge the first combination of the level set method and the sticky air approach.

This result does require high local mesh resolution in the order of 1 km or less near the air–lithosphere interface. In order to minimize CPU time, and yet maintain a small resolution around the lithosphere-sticky air interface, we investigated the possibility of reducing the thickness of the sticky air layer. This builds on the assumption that a certain thickness of the sticky air layer is required to ensure that the return flow in the air does not exert stress on the sticky air–lithosphere interface. The return flow is the result of the free slip top boundary condition (illustrated in Fig. 5a). Opening this top boundary, so making it a zero stress boundary which allows for through flow, makes the return flow within the sticky air layer disappear and strongly limiting the stress exerted on the interface (Fig. 5b). In Fig. 4b and c the results of six model runs are plotted. The models have either a 100 km, 50 km or a 25 km thick sticky air layer. All thicknesses were modeled with a free slip top boundary and an open top boundary. The semi-analytical solution from Crameri et al. (2012) is plotted as well. It illustrates that with a free slip top boundary a 100 km thick (and viscosity of 5 orders lower than

SED
6, 1523–1554, 2014

the lithosphere) sticky air layer is indeed needed to get satisfactory results. However for an open top boundary 100, 50 and 25 km of sticky air yield exactly the same result (the graphs overlap in Fig. 4b and c). The results also better match the semi-analytical solution than for 100 km sticky air and a free slip top boundary. All that is needed is a sufficiently thick sticky air layer for topography to build up. Topography variation on Earth rarely exceeds 10 km for which a sticky air layer of 25 km is by far sufficient and a further reduction in thickness is probably possible. Assuming constant resolution a removal of 75 km of air in a 800 km high model amounts to an approximate 10 % reduction in the number of elements. Further, as the red arrows illustrate in Fig. 5, the velocities with a free slip boundary are much larger in the air than for an open boundary. For an open boundary the time step (determined by CFL) can thus be larger.

4.3 Subduction benchmark

In this benchmark the partly subducted slab retreats and then sinks into the mantle due to its higher density than the mantle. There is no overriding plate. For comparison we look at the slab tip depth over time and compare the results of our model with those of six model runs from Schmeling et al. (2008) (Fig. 6a). These six models are the fastest and slowest models of three different viscosity averaging schemes for tracers (harmonic, geometric, arithmetic) discussed in detail in Schmeling et al. (2008). Our diffuse boundary method (see Sect. 2) for viscosity can best be compared with the geometric averaging method for tracers. Figure 6a shows that our slab sinks a little slower than the geometric averaging models. The averaging of viscosity is especially important for large viscosity contrasts of which there are two in the models of Schmeling et al. (2008): the air–slab interface and the small entrained air layer in the subduction zone (Figs. 7b and 9 of Schmeling et al., 2008). Both zones are important for the subduction velocity, the air–slab interface determines the decoupling between the two zones while a small entrained layer of air has a lubricating effect in the subduction zone. In our model the decoupling between slab and air is the same, but Fig. 7a illustrates that in our model due to the use of the level set method there is no entrainment of

SED
6, 1523–1554, 2014

air and therefore no artificial lubrication of the subduction zone. This explains why the sinking slab in our models is slightly slower than the geometric averaging model results from Schmeling et al. (2008).

4.4 Slab detachment

The target of the slab detachment benchmark is the timing and depth of slab detachment through viscous necking. Our results from two model runs with different mesh resolution are compared with results from the "$V \sim 100$, top layer model" from Schmalholz (2011). There is about two orders of magnitude difference in viscosity between the mantle and the location where necking occurs at startup. Figure 8 demonstrates resolution independence of our results and good agreement with the results from Schmalholz (2011). A particular result of using the level set method in monitoring slab necking is that the moment of final detachment is also recorded (intersection of the curve with the x-axis) as opposed to the data of Schmalholz (2011).

Figure 9 shows the time evolution of necking process where the acceleration of the process can readily be observed. In the first 17 Myr roughly half of the necking occurs while in the next 5 Myr it is completely detached. In the figures the thick white line represents the zero isocontour of the level set function. It is important to note that although the lithosphere has broken into two disjoint domains, it is still described by a single level set function. Using the data from Fig. 8, and because the location of the interface is exactly known, we can time the moment of detachment at 20.38 Myr.

5 Discussion and conclusions

The level set method is rarely used in geodynamical modeling. To investigate its applicability and benefits we have conducted four benchmarks highlighting different aspects of geodynamical multi-material flow modeling.

All the benchmarks show the accuracy of the level set method. Our results for the Rayleigh–Taylor instability benchmark agree well with results published by other groups using other methods. When compared to earlier level set method results from Bourgouin et al. (2006) and Samuel and Evonuk (2010) our results agree better with the original paper of Van Keken et al. (1997). With this benchmark we also demonstrate that the level set method is mass conservative. The accuracy of our method can also be observed in the subduction benchmark and the slab detachment benchmark as our results in these cases also match previously published results. For the post glacial rebound benchmark our results show an error of maximum 100 m with respect to the semi-analytical solution. This means we can resolve the long scale topography well within 10 % of our local finite element resolution. All benchmarks thus demonstrate the level set method to be accurate.

In several cases we demonstrate favorable properties of the level set method compared to tracer based methods. In the subduction benchmark we have shown that the level set method prevents entrainment of air into the subduction channel which otherwise would artificially lubricate the subduction zone. In the slab detachment benchmark we have demonstrated that the level set method can split from one bounded region into two bounded regions and accurately record the moment of detachment. In the post glacial rebound benchmark we illustrated that we match the semi-analytical solution using similar elemental resolutions as tracer-based methods. This further illustrates the statement of Zlotnik et al. (2008) that the level set method is favorable, particularly for 3-D applications, to the tracer method with regard to computational costs.

The level set function is chosen to be a signed distance function. This makes the implementation of a diffuse boundary method (Eq. 8) simple and the boundary width (h) easily adjustable. In the Rayleigh–Taylor instability benchmark we have shown that such a diffuse boundary method has a stabilizing effect on the results but does not alter them in any significant way.

SED
6, 1523–1554, 2014

With the post glacial rebound benchmark we demonstrated that the thickness of the sticky air layer can be reduced significantly when using a zero stress, free through-flow open top boundary resulting in an even better fit with the semi-analytical solution.

Overall we have shown that the level set method performs well and occasionally even better in geodynamical multi-material flow benchmarks and could therefore be considered as an alternative for tracer-based and phase field methods. For 3-D applications one can add to this the lower computational costs compared to tracer-based methods (Zlotnik et al., 2008).

Acknowledgements. We would like to thank Peter van Keken, Stephan Schmalholz, Fabio Crameri and Haro Schmeling for the fast sharing of data used in this paper. We acknowledge the Netherlands Research Institute of Integrated Solid Earth Sciences (ISES) for research funding and funding of computational support. This work was partly supported by the Research Council of Norway through its Centres of Excellence funding scheme, project number 223272.

References

Andrews, E. and Billen, M.: Rheologic controls on the dynamics of slab detachment, Tectonophysics, 464, 60–69, 2009. 1525

Androvičová, A., Čižková, H., and van den Berg, A.: The effects of rheological decoupling on slab deformation in the Earth's upper mantle, Stud. Geophys. Geod., 57, 460–481, 2013. 1525, 1528

Bangerth, W. and Heister, T.: ASPECT: Advanced Solver for Problems in Earth's ConvecTion, Texas A&M University/Computational Infrastructure in Geodynamics, 2013. 1532

Baumann, C., Gerya, T., and Connolly, J.: Numerical modelling of spontaneous slab breakoff dynamics during continental collision, Geological Society, London, Special Publications, 332, 99–114, 2010. 1525

Běhounková, M. and Čižková, H.: Long-wavelength character of subducted slabs in the lower mantle, Earth Planet. Sc. Lett., 275, 43–53, 2008. 1525

Billen, M. and Hirth, G.: Rheologic controls on slab dynamics, Geochem. Geophy. Geosy., 8, Q08012, doi:10.1029/2007GC001597, 2007. 1525

Bourgouin, L., Mühlhaus, H.-B., Hale, A., and Arsac, A.: Towards realistic simulations of lava dome growth using the level set method, Acta Geotech. Slov., 1, 225–236, doi:10.1007/s11440-006-0016-6, 2006. 1530, 1532, 1539

Braun, J., Thieulot, C., Fullsack, P., DeKool, M., Beaumont, C., and Huismans, R.: DOUAR: a new three-dimensional creeping flow numerical model for the solution of geological problems, Phys. Earth Planet. In., 171, 76–91, 2008. 1527

Brooks, A. and Hughes, T.: Stream-line upwind/Petrov–Galerkin formulation for convection dominated flows with particular emphasis on the incompressible Navier–Stokes equations, Comput. Methods Appl. Mech. Engrg., 32, 199–259, 1982. 1528

Chertova, M. V., Geenen, T., van den Berg, A., and Spakman, W.: Using open sidewalls for modelling self-consistent lithosphere subduction dynamics, Solid Earth, 3, 313–326, doi:10.5194/se-3-313-2012, 2012. 1528

Christensen, U.: The influence of trench migration on slab penetration into the lower mantle, Earth Planet. Sc. Lett., 140, 27–39, 1996. 1524

Čížková, H., van Hunen, J., and van den Berg, A.: Stress distribution within subducting slabs and their deformation in the transition zone, Phys. Earth Planet. In., 161, 202–214, 2007. 1528

Crameri, F., Schmeling, H., Golabek, G., Duretz, T., Orendt, R., Buiter, S., May, D. A., Kaus, B., Gerya, T., and Tackley, P.: A comparison of numerical surface topography calculations in geodynamic modelling: an evaluation of the "sticky air" method, Geophys. J. Int., 189, 38–54, doi:10.1111/j.1365-246X.2012.05388.x, 2012. 1526, 1527, 1531, 1532, 1536

Duretz, T., Gerya, T., and May, D.: Numerical modelling of spontaneous slab breakoff and subsequent topographic response, Tectonophysics, 502, 244–256, doi:10.1016/j.tecto.2010.05.024, 2011. 1525

Duretz, T., Schmalholz, S., and Gerya, T.: Dynamics of slab detachment, Geochem. Geophy. Geosy., 13, Q03020, doi:10.1029/2011GC004024, 2012. 1525

Duretz, T., Gerya, T. V., and Spakman, W.: Slab detachment in laterally varying subduction zones: 3-D numerical modeling, Geophys. Res. Lett., 41, 1951–1956, doi:10.1002/2014GL059472, 2014. 1525

Fullsack, P.: An arbitrary Lagrangian-Eulerian formulation for creeping flows and its application in tectonic models, Geophys. J. Int., 120, 1–23, 1995. 1527

Gerya, T., Fossati, D., Cantieni, C., and Seward, D.: Dynamic effects of aseismic ridge subduction: numerical modelling, Eur. J. Mineral., 21, 649–661, 2009. 1525

Gottlieb, S. and Shu, C.: Total variation diminishing Runge–Kutta schemes, Math. Comput., 67, 73–85, 1998. 1530
Gurnis, M. and Hager, B.: Controls of the structure of subducted slabs, Nature, 335, 317–321, 1988. 1524
Hale, A., Gottschaldt, K., Rosenbaum, G., Bourgouin, L., Bauchy, M., and Mühlhaus, H.: Dynamics of slab tear faults: insights from numerical modelling, Tectonophysics, 483, 58–70, 2010. 1527
Jiang, G. and Peng, D.: Weighted ENO schemes for Hamilton–Jacobi equations, SIAM J. Sci. Comput., 21, 2126–2143, 2000. 1530
Kronbichler, M., Heister, T., and Bangerth, W.: High accuracy mantle convection simulation through modern numerical methods, Geophys. J. Int., 191, 12–29, 2012. 1526
Lenardic, A. and Kaula, W.: A numerical treatment of geodynamic viscous flow problems involving the advection of material interfaces, J. Geophys. Res., 98, 8243–8260, doi:10.1029/92JB02858, 1993. 1526
Magni, V., van Hunen, J., Funiciello, F., and Faccenna, C.: Numerical models of slab migration in continental collision zones, Solid Earth, 3, 293–306, doi:10.5194/se-3-293-2012, 2012. 1525
Min, C.: On reinitializing level set functions, J. Comput. Phys., 229, 2764–2772, doi:10.1016/j.jcp.2009.12.032, 2010. 1529
Oka, H. and Ishii, K.: Numerical analysis on the motion of gas bubbles using level set method, J. Phys. Soc. Jpn., 68, 823–832, 1999. 1527
Osher, S. and Fedkiw, R.: Level set methods: an overview and some recent results, J. Comput. Phys., 169, 463–502, doi:10.1006/jcph.2000.6636, 2001. 1527, 1528, 1529
Osher, S. and Sethian, J.: Fronts propagating with curvature-dependent speed: algorithms based on Hamilton-Jacobi formulations, J. Comput. Phys., 79, 12–49, doi:10.1016/0021-9991(88)90002-2, 1988. 1528
Osher, S. and Shu, C.-W.: High-order essentially non-oscillatory schemes for Hamilton–Jacobi equations, SIAM J. Numer. Anal., 28, 907–922, 1991. 1530
Quinquis, M., Buiter, S., and Ellis, S.: The role of boundary conditions in numerical models of subduction zone dynamics, Tectonophysics, 497, 57–70, doi:10.1016/j.tecto.2010.11.001, 2011. 1525
Rao, R., Mondy, L., Noble, D., Moffat, H., D. B., A., and Notz, P.: A level set method to study foam processing: a validation study, Int. J. Numer. Meth. Fl., 68, 1362–1392, 2011. 1527

Samuel, H. and Evonuk, M.: Modeling advection in geophysical flows with particle level sets, Geochem. Geophy. Geosy., 11, Q08020, doi:10.1029/2010GC003081, 2010. 1532, 1535, 1539, 1545

Schmalholz, S.: A simple analytical solution for slab detachment, Earth Planet. Sc. Lett., 304, 45–54, 2011. 1532, 1534, 1538

Schmeling, H., Babeyko, A., Enns, A., Faccenna, C., Funiciello, F., Gerya, T., Golabek, G., Grigull, S., Kaus, B., and Morra, G.: A benchmark comparison of spontaneous subduction models – towards a free surface, Phys. Earth Planet. In., 171, 198–223, 2008. 1525, 1527, 1531, 1532, 1533, 1537, 1538

Segal, A. and Praagman, N.: The SEPRAN package. Technical report, Technical, Ingenieurs-Bureau Sepra, the Netherlands, available at: http://ta.twi.tudelft.nl/sepran/sepran.html, 2005. 1527

Sussman, M., Fatemi, E., Smereka, P., and Osher, S.: A level set approach for computing solutions to incompressible two-phase flow II, in: Proceedings of the Sixth International Symposium on Computational Fluid Dynamics, Lake Tahoe, NV, 1995. 1529

Tackley, P. and King, S.: Testing the tracer ratio method for modeling active compositional fields in mantle convection simulations, Geochem. Geophy. Geosy., 4, 8302, doi:10.1029/2001GC000214, 2003. 1525, 1526, 1532

Thieulot, C.: FANTOM: two- and three-dimensional numerical modelling of creeping flows for the solution of geological problems, Phys. Earth Planet. In., 188, 47–68, 2011. 1527

Thieulot, C.: ELEFANT: a user-friendly multipurpose geodynamics code, submitted, Solid Earth, 2014. 1545

Thieulot, C., Glerum, A., Hillebrand, B., Spakman, W., and Torsvik, T.: Multiphase geodynamical modelling using Aspect, in preparation, 2014a. 1535

Thieulot, C., Schmalholz, S., Glerum, A., Hillebrand, B., and Spakman, W.: A two- and three-dimensional numerical comparison study of slab detachment, in preparation, 2014b. 1534

van Hunen, J. and Allen, M.: Continental collision and slab break-off: a comparison of 3-D numerical models with observations, Earth Planet. Sc. Lett., 302, 21–37, doi:10.1016/j.epsl.2010.11.035, 2011. 1525

van Hunen, J. and van den Berg, A.: Plate tectonics on the early Earth: limitations imposed by strength and buoyancy of subducted lithosphere, Lithos, 103, 217–235, 2008. 1525, 1528

SED

6, 1523–1554, 2014

Geodynamical modeling using the level set method

B. Hillebrand et al.

Van Keken, P., King, S., Schmeling, H., Christensen, U., Neumeister, D., and Doin, M.: A comparison of methods for the modeling of thermochemical convection, J. Geophys. Res.-Sol. Ea., 102, 22477–22495, 1997. 1526, 1532, 1534, 1535, 1539, 1545

Zlotnik, S., Fernandez, M., Diez, P., and Verges, J.: Modelling gravitational instabilities: slab break–off and Rayleigh–Taylor diapirism, Pure Appl. Geophys., 165, 1491–1510, doi:10.1007/s00024-004-0386-9, 2008. 1527, 1539, 1540

SED

6, 1523–1554, 2014

Table 1. Table containing the timing and hight (max v_{rms}) of the first peak of our model runs and selected others from the literature.

method (code)	grid	t_1	v_1	source
Tracers (ELEFANT)	400 × 400	208.7	0.003093	Thieulot (2014)
Marker chain	30 × 30	213.38	0.00300	PvK in
	50 × 50	211.81	0.003016	Van Keken et al. (1997)
	80 × 80	210.75	0.003050	
level set	60 × 60	228.88	0.002925	Samuel and Evonuk (2010)
	120 × 120	215.87	0.003051	
	240 × 240	211.52	0.003093	
particle level set	60 × 60	215.57	0.003087	
	120 × 120	212.22	0.003109	
level set (SEPRAN)	60 × 60	213.03	0.003091	this study
	160 × 160	209.21	0.003096	
	240 × 240	209.19	0.003095	

SED
6, 1523–1554, 2014

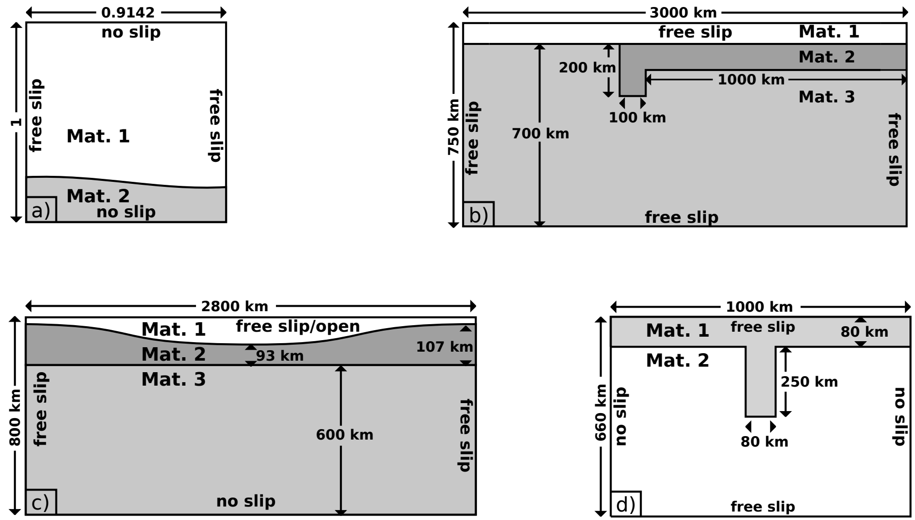

Figure 1. (a) Setup for the Rayleigh–Taylor instability benchmark. Material 1 has $\eta = 100\,\mathrm{Pa\,s}$ and $\rho = 1010\,\mathrm{kg\,m^{-3}}$. Material 2 has $\eta = 100\,\mathrm{Pa\,s}$ and $\rho = 1000\,\mathrm{kg\,m^{-3}}$. **(b)** Setup for the subduction benchmark. Material 1 is a sticky air layer with $\eta = 10^{18}\,\mathrm{Pa\,s}$ and $\rho = 0\,\mathrm{kg\,m^{-3}}$, material 2 is a slab with $\eta = 10^{23}\,\mathrm{Pa\,s}$ and $\rho = 3300\,\mathrm{kg\,m^{-3}}$ and material 3 is the mantle with $\eta = 10^{21}\,\mathrm{Pa\,s}$ and $\rho = 3200\,\mathrm{kg\,m^{-3}}$. **(c)** Setup for the post glacial rebound benchmark. Material 1 is a sticky air layer with $\eta = 10^{18}\,\mathrm{Pa\,s}$ and $\rho = 0\,\mathrm{kg\,m^{-3}}$. Material 2 is a lithosphere with $\eta = 10^{23}\,\mathrm{Pa\,s}$ and $\rho = 3300\,\mathrm{kg\,m^{-3}}$ and material 3 is the mantle with $\eta = 10^{22}\,\mathrm{Pa\,s}$ and $\rho = 3300\,\mathrm{kg\,m^{-3}}$. **(d)** Setup for the detachment benchmark. Material 1 is a slab with non linear rheology and $\rho = 3300\,\mathrm{kg\,m^{-3}}$ and material 2 is the mantle with $\eta = 10^{21}\,\mathrm{Pa\,s}$ and $\rho = 3150\,\mathrm{kg\,m^{-3}}$.

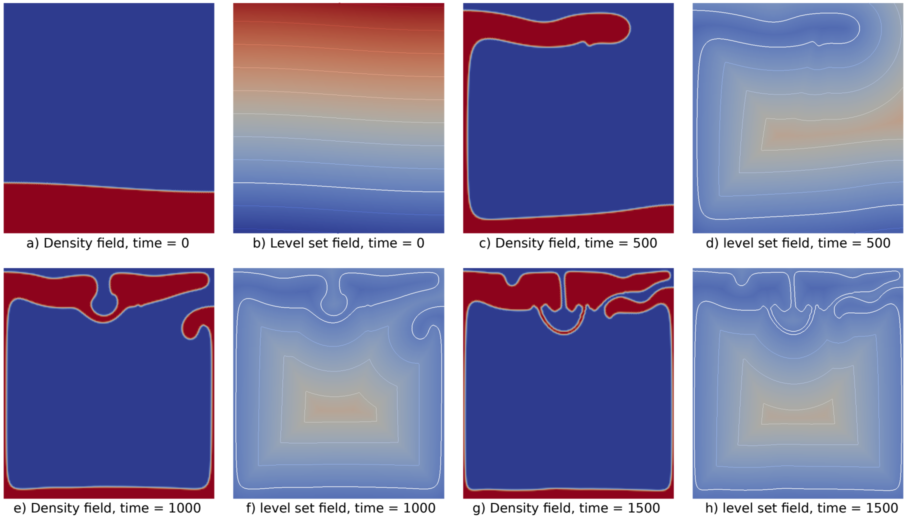

Figure 2. Snapshots of the evolution of the density field and the level set field with time. Level set isocontours are plotted every 0.1. The thick white line represents 0.

SED
6, 1523–1554, 2014

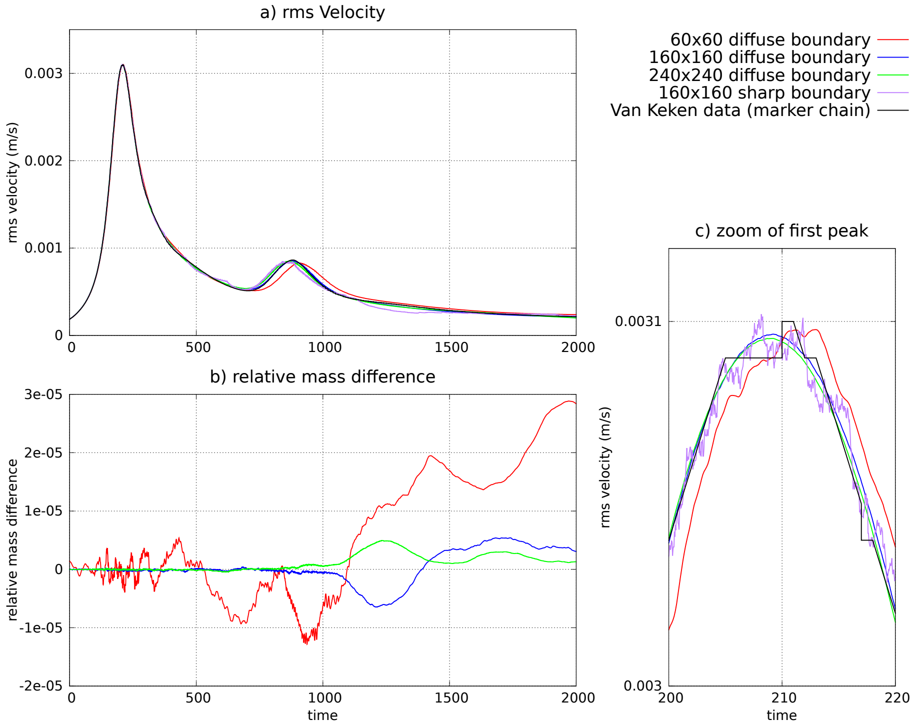

Figure 3. (a) Root mean square velocity of the entire domain. The van Keken data is the data from the marker chain method of van Keken from the original article. **(b)** The relative mass difference over time according to Eq. (12). **(c)** A zoom-in of the first peak in the rms velocity plot of **(a)**.

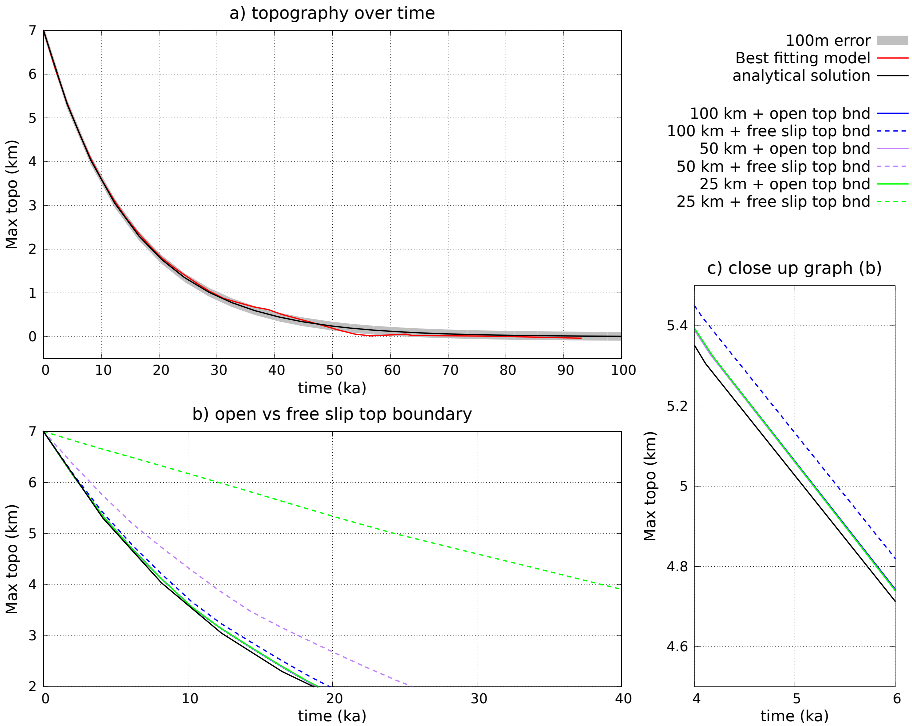

Figure 4. (a) The topography over time of our best fitting model run. **(b)** The data of open vs. free slip top boundaries for different sized sticky air layers. The solid green, purple and blue line exactly overlap. Confirmed by the close-up in **(c)**. **(c)** Contains a close-up of **(b)** showing that the three open boundary model runs (solid lines) do indeed yield exactly the same result.

SED
6, 1523–1554, 2014

Geodynamical modeling using the level set method

B. Hillebrand et al.

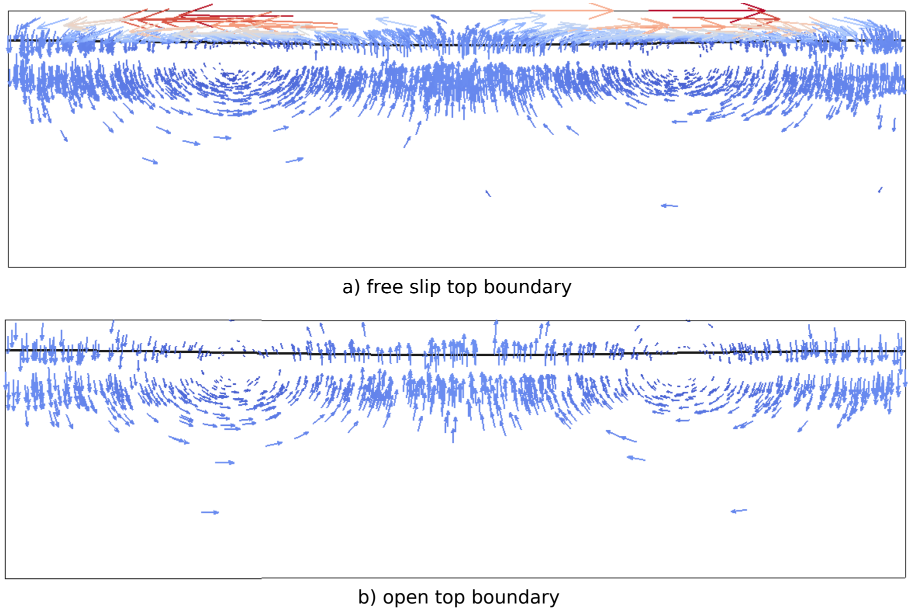

Figure 5. Flow field in a model with a free slip top boundary **(a)** and with an open top boundary **(b)**. The arrows are scaled in the same way, both in length and color. The black line denotes the zero level set and thus the surface topography.

SED
6, 1523–1554, 2014

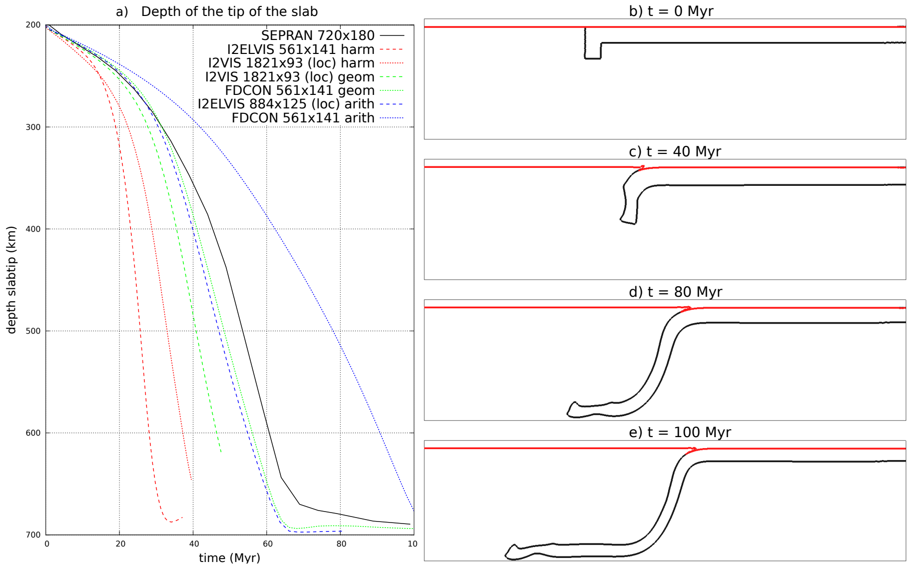

Figure 6. (a) Depth of slab tip vs. time. **(b)** through **(e)** Snapshots in time of the slab. The red line indicates the location of the zero isocontour of the level set function tracking the surface and the black line indicates the zero isocontour of the level set function tracking the slab.

SED
6, 1523–1554, 2014

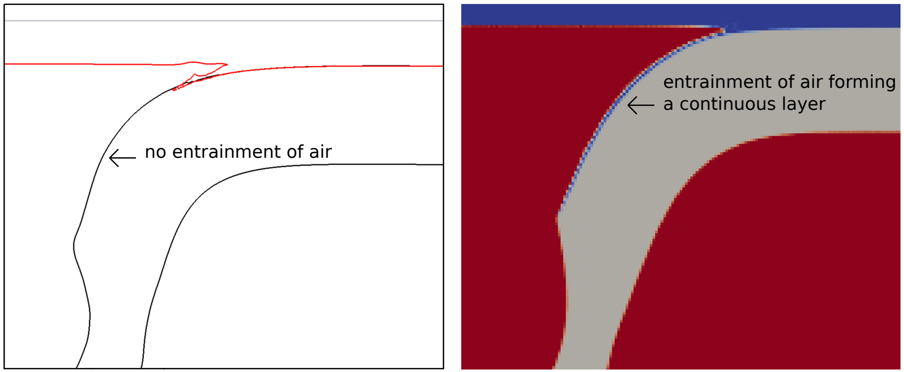

Figure 7. Comparison of the entrainment of air between a tracer based method (ELEFANT) and our level set method.

SED
6, 1523–1554, 2014

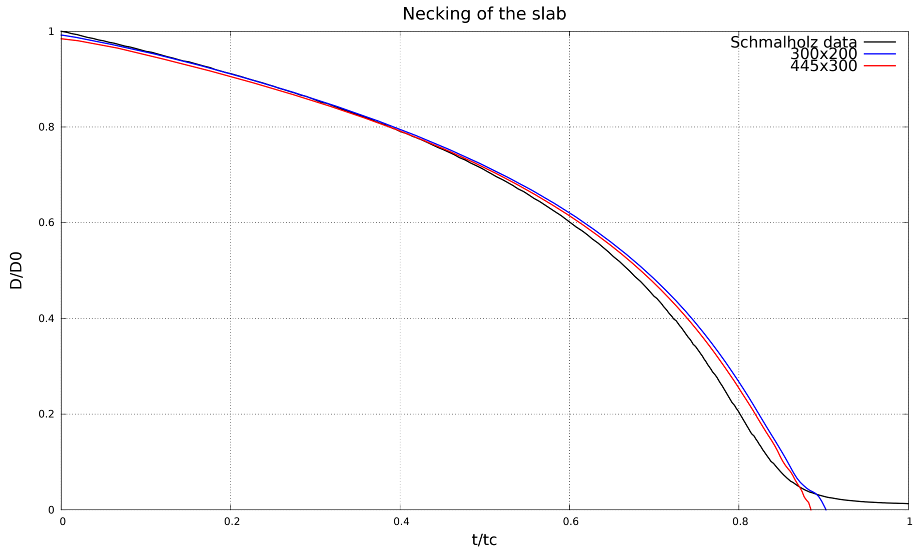

Figure 8. The necking instability over time.

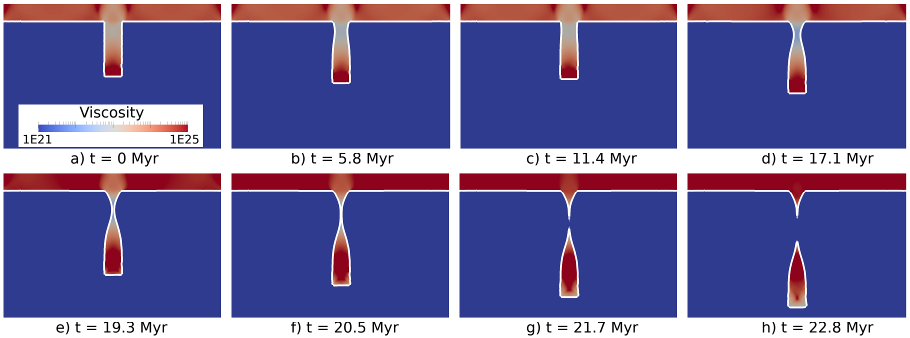

Figure 9. Snapshots of viscosity during the necking process. The white line indicates the zero isocontour of the level set function. Nte that the frames are plotted with different time intervals to demonstrate the acceleration of slab necking.

SED
6, 1523–1554, 2014